Enhancement in electroluminescence of PLED by optimizing coating parameters and inserting an injection layer

S. H. YANG*, H. J. HSIEH, D. W. ZHUANG, T. Y. CHEN
Department of Electronic Engineering, National Kaohsiung University of Applied Sciences, Kaohsiung, Taiwan, R.O.C.

For polymer light-emitting diode (PLED), the luminance properties of device are determined by the device structure and the morphology and thickness of the organic layer. Accordingly, this study investigates the electroluminescence (EL) enhancement of the PLED by optimizing the coating parameters and inserting an electron injection layer. Poly(3,4-ethylenedioxythiophene):poly(styrene sulfonate) (PEDOT:PSS) and poly(9,9-dihexylfluorene-2,7-diyl) (PDHF) were used as the conductive layer and the emission layer materials, respectively. The PLED structure was indium tin oxide/PEDOT:PSS/PDHF/Al. The low turn-on voltage and the enhanced EL intensity of the PLED were resulted from the improved carrier balance and recombination in the PDHF emission layer. When a LiF layer was inserted between the PDHF layer and the Al cathode, the EL intensity of the PLED was enhanced because of the increase in electron injection. In this condition, the maximum EL intensity of 45.8 cd/m^2 at 13 V was obtained, which was 1.96 times higher than that in the case of the device without a LiF layer.

(Received March 3, 2011; accepted March 16, 2011)

Keywords: Electroluminescence, Tunneling effect, Injection layer

1. Introduction

Polymer light-emitting diodes (PLEDs) were first studied by Burroughes et al. in 1990; since then, PLEDs have been extensively developed because of their potential application in full-color, flat-panel, high-definition displays [1-3]. In a PLED, light emission occurs via a radiative recombination by electrical excitation, which is an electroluminescence (EL) phenomenon. That is, the PLED converts electrical energy into photon emission. The emission wavelength is dependent on the properties of the emitting material.

Inasmuch as the development of PLEDs is highly anticipated, the demand for improving the performance of the device is growing. In recent years, the carrier balance and the efficiency of PLEDs have been improved by using highly efficient emission materials [4,5] and preparing PLEDs with a stacking layer structure in which a hole transport layer and an electron blocking layer are deposited [6-10]. Another interesting approach involves applying nanotechnology to the PLED in order to enhance the luminance of the PLED; in this approach, inorganic quantum-dot nanoparticles are mixed with the polymer matrix or used as a buffer layer [11-14]. By controlling the dimension and morphology of the nanoparticles, the recombination of carriers is increased owing to the quantum confinement effect, and a low operating voltage and high efficiency of the PLED is achieved. In addition, a modified spin-coating process is presented, which is a solution process for PLED fabrication; in this process, the substrate is placed at an appropriate position with respect to the center of spinner, consequently, the light emission uniformity and efficiency of the PLED are improved [15]. This modified spin-coating process allows the PLED being prepared on a flexible substrate. It is also easy to modify the morphology and thickness of a polymer film by altering the solvent species, solution concentration, spinning speed, and baking temperature. Therefore, this process offers a great potential for the development of thin, light-weight, large-sized PLEDs.

Although the solution-processable PLED shows great promise for commercialization, the morphology and interfaces between the films, which determine the efficiency of a device, are of vital importance. Therefore, in this study, the EL intensity of the PLED was enhanced by optimizing the spin-coating parameters of the spin speed and the baking temperature. In addition, a LiF electron injection layer was prepared to improve the carrier recombination. The luminescence properties of the emission layer and the EL properties of the PLED were investigated.

2. Experimental

For the light-emitting substances, poly(alkylfluorene)s (PFs) are one of the most promising materials that can be used for the fabrication of PLEDs [16,17]. By incorporating various types of comonomers, we can effectively tune the emission color of PFs to cover the entire visible-light region [18]. The poly(9,9-dihexylfluorene-2,7-diyl) (PDHF) is a type of PFs that has a bluish-green emission color [19].

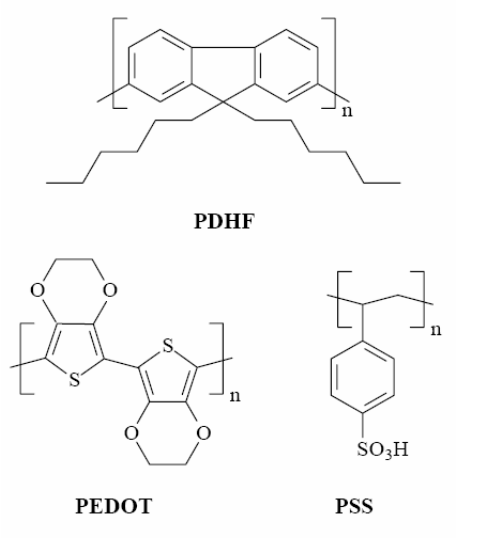

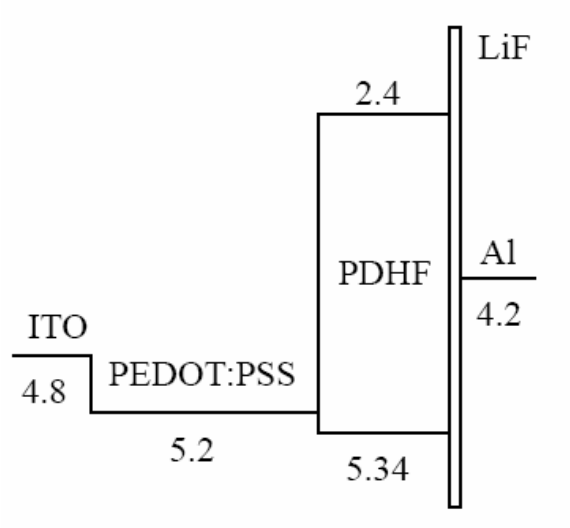

Fig. 1. Chemical structures of organic materials and energy-level diagram of the bluish-green PLED.

In this work, PDHF and poly(3,4-ethylene dioxythiophene):poly(styrene sulfonate) (PEDOT:PSS) were selected as the emission layer and the conductive layer materials, respectively; they were used as received from commercial sources without further purification. PEDOT:PSS with the highest occupied molecular orbital (HOMO) of around 5.2 eV is a common p-type conductive polymer, which contains a heterocyclic thiophene ring bridged by a diether. Figure 1 shows the chemical structures of the organic materials used in this investigation. An indium tin oxide (ITO)-coated glass with a resistivity of 15 Ω per square was used as the substrate. The PLED structure was ITO/PEDOT:PSS/PDHF/Al. First, the ITO surface was cleaned with an organic solvent and was then dried using high purity nitrogen gas. After that, PEDOT:PSS (2.8% water dispersion) was spin-coated on ITO at 8000 rpm and then baked at 130°C for 40 min; this 100-nm-thick PEDOT:PSS film functioned as a hole injection/transport layer. The PDHF emitting layer, with a glass transition temperature (T_g) of around 65°C, was prepared on PEDOT:PSS by spin-coating with the PDHF solution (0.5 wt%, dissolved in tetrahydrofuran (THF)) at spin speeds of 1000–9000 rpm. It was then baked at 45, 60, and 75°C for 30 min in atmosphere. The annealing process could improve the adhesion, the morphology, and the chain conformation of the polymer film [20-22]. The thicknesses of the PDHF layer were about 119–257 nm. Finally, an Al electrode (200 nm) was deposited on the PDHF layer by evaporation under a pressure of 5×10^{-6} torr. The active area of the PLED was 12 mm^2.

The surface roughness was evaluated by using an atomic force microscope (AFM), and the film thickness was measured with a scanning electron microscope (SEM, Hitachi S3000N). The ionization potential of PDHF was measured by using the cyclic voltammetry (CV) method. The absorption spectra were measured by a Hitachi U-2800 spectrophotometer, and the effects of spin speed and baking temperature on the photoluminescence (PL) property of the PDHF film were evaluated using a Hitachi F-4500 fluorescence spectrophotometer equipped with a 150 W xenon lamp. For EL measurements, a Keithley 2410 programmable voltage-current source was used, and the luminance and Commission Internationale del'Eclairage (CIE) coordinates were estimated using the Minolta Chroma Meter CS-100A. The EL spectra were measured using the Newport OSM-400 spectrophotometer. All measurements were carried out at room temperature in air without encapsulating the devices. Nevertheless, because the devices were not encapsulated, the stability and lifetime of the PLED were not evaluated.

3. Results and discussion

The energy-level diagram of the bluish-green PLED is shown in Fig. 1. The HOMO and the lowest unoccupied molecular orbital (LUMO) of each layer are aligned with respect to the vacuum level. Empirically, a nonuniform ITO surface would result in a poor injection of holes. Therefore, in this study, the ITO surface was smoothened by spin-coating a thin PEDOT:PSS conductive layer. As a result, the hopping of holes from ITO to the PDHF layer was improved and the tunneling effect was reduced.

The absorption and PL spectra of the PDHF film

baked at different temperatures are shown in Fig. 2. The PDHF film showed a maximum absorption at 380 nm, which was attributed to the π–π* transition of the electrons. For the PDHF film baked at 45–75°C, the bluish-green PL spectrum of the PDHF excited at 380 nm revealed a maximum PL peak at 423 nm and a well-defined vibronic feature at 450 nm. The maximum PL peak was attributed to the intrachain emission, where the electrons were transited from the excited state S_10 to the ground state S_00. The vibronic features for peaks at 450, 490, and 535 nm were attributed to the aggregative (excimer) emissions, in which the electron transitions were from the excited state S_10 to the ground states of S_01, S_02, and S_03, respectively. The excimer emission was caused by an increase in the aggregation of chromophores. This intermolecular interaction resulted in an energy band separation and emissions at longer wavelengths [23]. It was also found that the conformational states formed during spin coating were thermodynamically unstable and changed with baking temperatures. The interchain emission was more reactive with temperature variation than the intrachain emission, which led to the alternation of the PL intensity. The maximum PL intensity was obtained when the PDHF film was baked at 60°C. However, when the baking temperature was higher than T_g, the polymer chains began to relax and tended to aggregate. Further, the rapid evaporation of the solvent caused the formation of many hollows or free volumes in the film, which roughened the surface morphology and facilitated the extension of the polymer chains. The surface roughness of the PDHF layer measured by AFM was 2.40, 1.16, and 5.13 nm at baking temperatures of 45, 60 and 75°C, respectively. In addition, when the polymer film was baked at a temperature higher than T_g, low-emission materials, i.e., plastic substances, were formed, and as a result, the PL intensity was quenched [2,3].

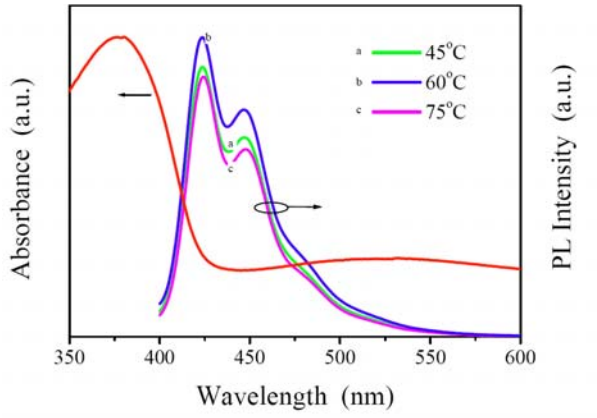

Fig. 2. Absorption and PL spectra of the PDHF film baked at different temperatures.

Empirically, the main chain and functional groups moved freely because of the heat treatment, nevertheless, the packing density and surface morphology of the PDHF polymer changed. Such changes influenced the thermal expansion of the polymer. A higher baking temperature generated a lower tensile stress in the film, which led to the polymer film being more relaxed. Therefore, when the polymer films were baked at an appropriate temperature, the PLED acquired a better dimensional stability against thermal breakdown at the polymer–cathode or polymer–anode interface. The effect of the baking temperature on the performance of the PLED in terms of the relationship between current and voltage is shown in Fig. 3. In this study, the turn-on voltage of the PLED was defined when an electric current of 1 mA (8 mA/cm^2) was achieved, although the turn-on voltage was defined for the voltage to reach a current density of 1 mA/cm^2 or a luminance of 1 or 10 cd/m^2 [24-28]. It was found that the turn-on voltage of the PLED for the PDHF film baked at 45, 60, and 75°C was 2.11, 1.35, and 1.52 V, respectively. The low turn-on voltage of the PLED for PDHF film baked at 60°C revealed that the injection of the minority carriers, i.e., electrons, was enhanced because of the improved morphology of the PDHF film and the mended interface states between layers.

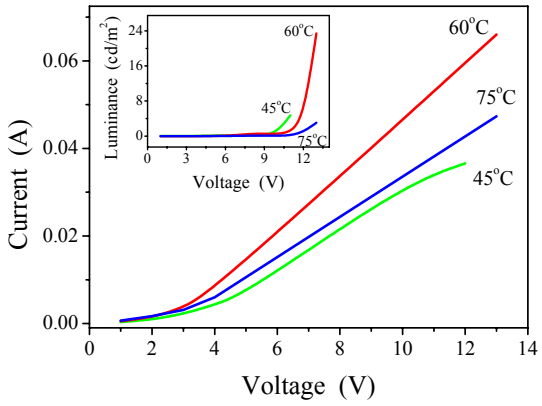

Fig. 3. Current–voltage characteristics of the PLED for PDHF film annealed at 45, 60, and 75°C for 30 min.

The inset of Fig. 3 shows that the optimum performance of the PLED was achieved when the PDHF film was baked at an appropriate temperature of 60°C. This was attributed to the fact that the packing density of the PDHF film was enhanced when it was baked at a temperature lower than T_g. The ability to endure the Joule heat generated during the operation of the PLED was enhanced; and the thermal stability of the polymer film was improved; hence, the increased lifetime of the PLED film was expected. The decreased luminance of the PLED for PDHF baked at 75°C was attributed to the increased interaction between polymer chains, which was induced by the change in the chain conformation [29]. To enhance the exciton confinement, the intermolecular interaction has to be minimized.

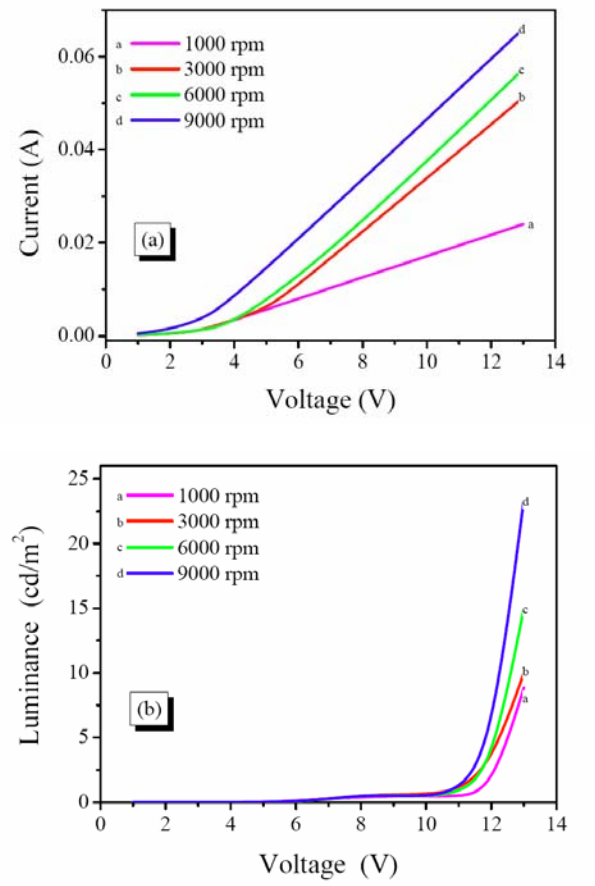

Fig. 4. Dependences of (a) I-V and (b) L-V characteristics of the PLED for PDHF prepared at spin speeds of 1000−9000 rpm and baked at 60 °C for 30 min.

Fig. 4(a) shows the dependence of the current-voltage (I-V) characteristics of the PLED for PDHF prepared at spin speeds of 1000–9000 rpm and baked at 60°C for 30 min. A low spin speed caused the coiling of polymer chains; as a result, the injection and transport of electrons were blocked. In contrast, a high spin speed led to the extension of the polymer chains, which would facilitate the injection and transfer of electrons. Hence, the electric current of the PLED increased with an increase in the spin speed. In addition, the centrifugal force was increased at a high spin speed; consequently, the coating solution overcame the adhesive force of the ITO surface to form a thinner polymer film. Figs. 5(a)−(d) show the SEM cross section images of the PDHF film prepared at different spin speeds. A PDHF film with a smooth surface was observed. The thickness of the PDHF film at spin speeds of 1000, 3000, 6000, and 9000 rpm was 257, 208, 168 and 119 nm, respectively. By increasing the spin speed, a thin and smooth PDHF film was obtained, which resulted in a low turn-on voltage of the PLED.

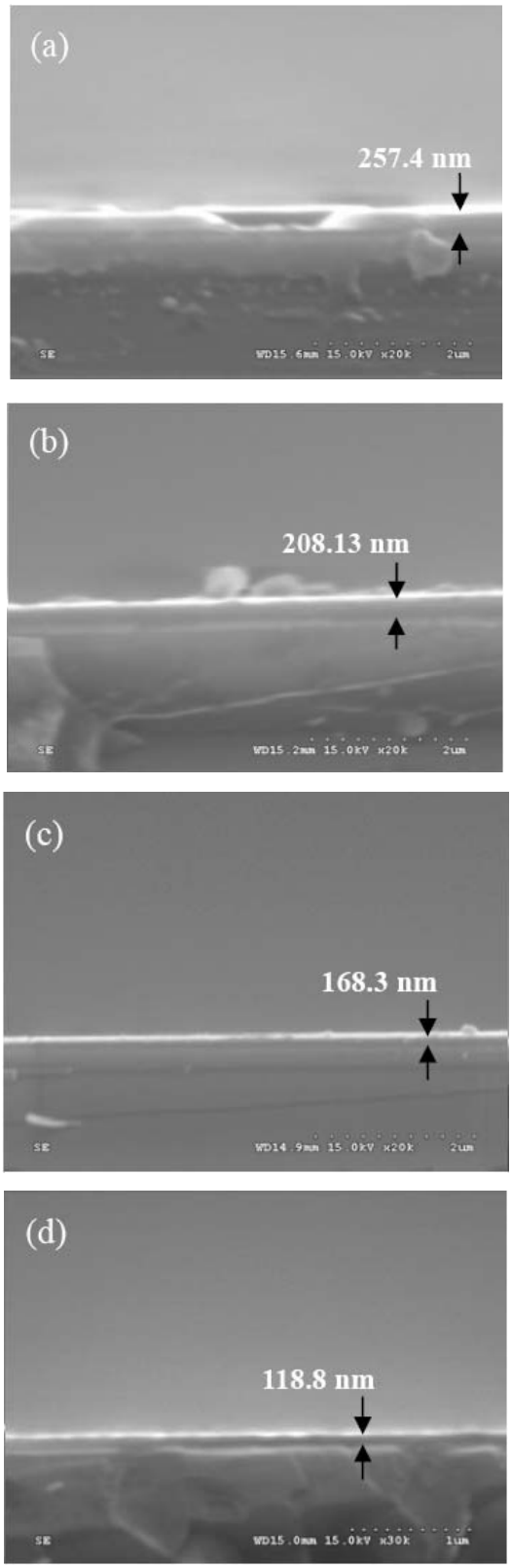

Fig. 5. SEM cross sectional micrographs of the PDHF film prepared at spin speeds of (a) 1000, (b) 3000, (c) 6000, and (d) 9000 rpm.

The luminance-voltage (L-V) relationship of the PLED for the PDHF film prepared at different spin speeds and baked at 60°C for 30 min is shown in Fig. 4(b). For the PDHF film prepared at low spin speeds, the interaction force between the interchains was stronger than the centrifugal force. Because of this intermolecular aggregation, a poor EL intensity of the PLED was observed [30]. Hence, a high luminance and better quality of the PDHF film was obtained when the film was prepared at a high spin speed. The optimum luminance of the PLED was achieved when the PDHF film was prepared at a spin speed of 9000 rpm; this was attributed to the improved carrier balance and the enhanced recombination in the thin and smooth PDHF emitting layer. The maximum luminance of 23.4 cd/m^2 was obtained at an applied voltage of 13 V and a current of 68 mA.

Fig. 6 shows the EL spectra of the PLED for the PDHF layer prepared at different spin speeds. The EL spectra consisted of two emission peaks at around 423 and 500 nm. The dominant emission peak at 500 nm was attributed to the excimer emission. The EL intensity of the PLED was enhanced by increasing the spin speed for the PDHF preparation; this result was consistent with the L-V analyses, as shown in Fig. 4(b).

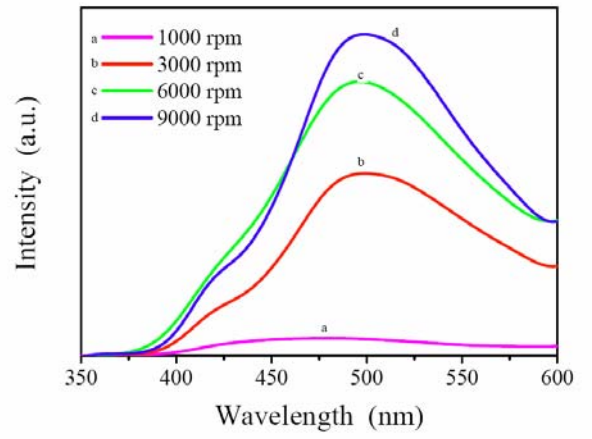

Fig. 6. EL spectra of the PLED for PDHF film prepared at different spin speeds.

For enhancing the luminance of the PLED, a thin LiF insulating layer was thermally deposited between the PDHF layer and the Al cathode; its thickness was measured by using an oscillating crystal monitor. LiF is an ionic-crystalline material, which can increase the injection of tunneling electrons from the metal cathode to the emitting layer [31-33]; the tunneling probability of electrons is dependent on the thickness of the LiF layer, the difference in the barrier height between the layers, and the electric field strength of the device. Figure 7 shows the EL properties of the PLED for the structure of ITO/PEDOT (100 nm)/PDHF (119 nm)/LiF (x)/Al (200 nm), where the values of x were varied from 0 to 1 nm. It was found that the turn-on voltage of the PLED increased with an increase in the thickness of the LiF layer because a thick LiF layer functioned as a barrier layer and reduced the injection of electrons from the Al cathode to the PDHF emitting layer. However, the current of the PLED increased with an increase in the applied voltage because of the increase in the electric field strength. Figure 7(b) shows the L-V characteristics of the PLED. The luminance of the PLED shows a significant change with the thickness of the LiF layer.

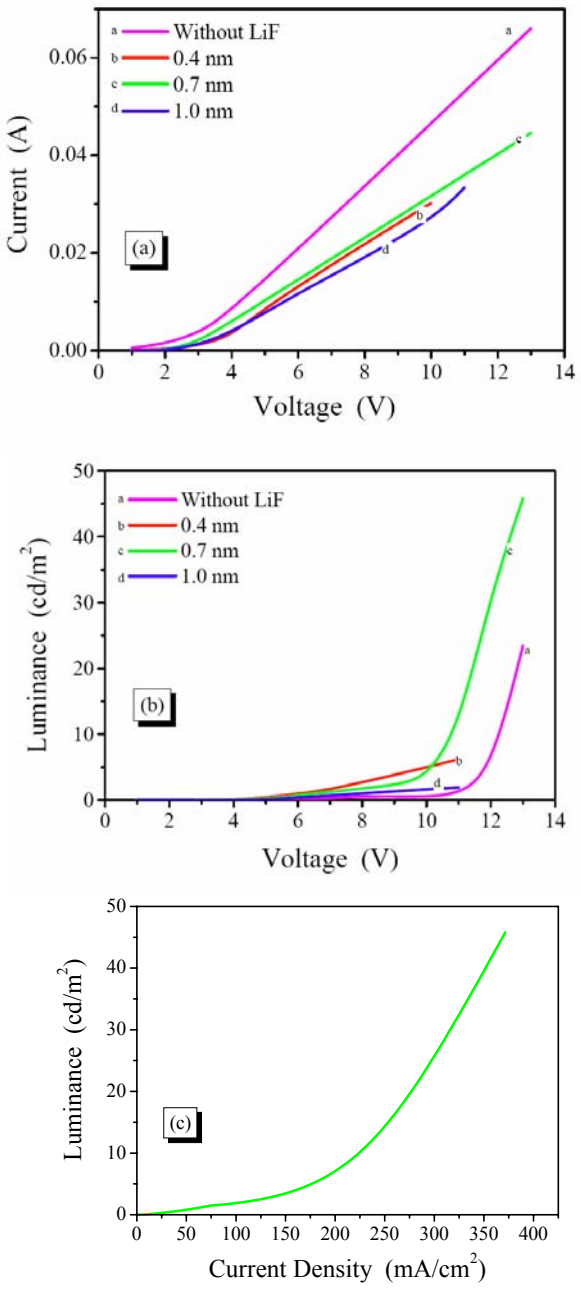

Fig. 7. (a) I-V and (b) L-V characteristics of the PLED inserted with LiF layer with different thicknesses; (c) L-J Plot of the PLED for LiF layer thickness of 0.7 nm.

The luminance of the PLED was low when the thickness of the LiF layer was less than 0.4 nm, which was attributed to the fact that more electrons were trapped at the PDHF/LiF interface. A significant enhancement in the luminance of the PLED was obtained when the thickness of the LiF layer was 0.7 nm. At this LiF thickness, the injection of electrons tunneling through the LiF layer increased and the carrier balance and recombination in the PDHF emitting layer improved; consequently, the luminance of the PLED improved. Nevertheless, when the thickness of the LiF layer was more than 1 nm, the tunneling probability of electrons from the cathode to the emitting layer decreased, leading to a decrease in the luminance of the PLED. On a PLED with a 0.7-nm-thick LiF layer, a low turn-on voltage of 5 V was measured; and the maximum luminance of 45.8 cd/m^2 at 13 V was obtained with CIE coordinates of (0.23, 0.33). The EL intensity has enhanced by a factor of 1.96 when the PLED was prepared with a LiF layer. The luminance-current density plot of the PLED for LiF layer thickness of 0.7 nm is presented in Fig. 7(c). Luminance of the PLED was increased with the increase of current density.

4. Conclusions

For the PDHF, the maximum absorption peak was at 380 nm, and a dominant emission peak at 423 nm together with a vibronic feature at 450 nm was observed from the PL measurement. The low turn-on voltage of the PLED for the PDHF film baked at 60°C suggests that the injection of electrons was enhanced due to the improved morphology of PDHF and the mended interface states between the films. Meanwhile, in the case of the PDHF film prepared at a high spin speed, the improvements in carrier balance and recombination in the thin and smooth PDHF film led to the low turn-on voltage and the increased current of the PLED. The maximum luminance of 23.4 cd/m^2 was achieved at 13 V. A significant enhancement in the luminance of the PLED was obtained when a 0.7-nm-thick LiF layer was inserted between the PDHF and the Al cathode to increase the tunneling injection of electrons; the maximum luminance of 45.8 cd/m^2 was obtained at 13 V, with CIE coordinates at (0.23, 0.33).

Acknowledgements

The authors would like to express their sincere gratitude to the National Science Council of the Republic of China for financially supporting this work under contract No. NSC 99-2221-E-151-038.

References

[1] J. H. Burroughes, D. D. C. Bradley, A. R. Brown, R. N. Marks, K. Mackay, R. H. Friend, P. L. Burns, A. B. Homes, Nature **347**, 539 (1990).
[2] T. K. Chuang, M. Troccoli, P. C. Kuo, A. Jamshidi-Roudbari, M. Hatalis, A. T. Voutsas, T. Afentakis, Electrochem Solid-State Lett. **10**, J92 (2007).
[3] M. Troccoli, T. K. Chuang, A. Hamshidi, P. C. Kuo, J. Spirko, M. Hatalis, A. T. Voutsas, T. Afentakis, J. Hartzell, ECS Trans. **3**, 237 (2006).
[4] J. C. Sánchez, M. Estrada, Microelectron. Reliab. **49**, 1503 (2009).
[5] J. Sun, J. Chen, J. Zou, S. Ren, H. Zhong, D. Zeng, J. Du, E. Xu, Q. Fang, Polymer **49**, 2282 (2008).
[6] Y. Aoki, M. Shakutsui, K. Fujita, Thin Solid Films **518**, 493 (2009).
[7] M. Shakutsui, H. Matsuura, K. Fujita, Org. Electron. **10**, 834 (2009).
[8] A. C. Rabelo, A. Marletta, R. A. Silva, N. M. Barbosa, O. L. Bottecchia, Synth. Met. **159**, 2318 (2009).
[9] D. Madhwal, S. S. Rait, A. Verma, A. Kumar, P. K. Bhatnagar, P. C. Mathur, M. Onoda, J. Lumin. **130**, 331 (2010).
[10] H. Wu, J. Zou, D. An, F. Liu, W. Yang, J. Peng, A. Mikhailovsky, G. C. Bazan, Y. Cao, Org. Electron. **10**, 1562 (2009).
[11] S. N. Hsieh, T. C. Wen, T. F. Guo, Mater. Chem. Phys. **101**, 383 (2007).
[12] S. A. Carter, J. C. Scott, P. J. Brock, Appl. Phys. Lett. **71**, 1145 (1997).
[13] I. Ugarte, W. Cambarau, C. Waldauf, F. L. Arbeloa, Org. Electron. **10**, 1606 (2009).
[14] S. O. Jeon, K. S. Yook, J. Y. Lee, Synth. Met. **160**, 39 (2010).
[15] Q. Niu, Y. Shao, W. Xu, L. Wang, S. Han, N. Liu, J. Peng, Y. Cao, J. Wang, Org. Electron. **9**, 95 (2008).
[16] A. W. Grice, D. D. C. Bradley, M. T. Bernius, M. Inbasekaran, W. W. Wu, E. P. Woo, Appl. Phys. Lett. **73**, 629 (1998).
[17] M. Kreyenschmidt, G. Klaerner, T. Fuhrer, J. Ashenhurst, S. Karg, W. D. Chen, V. Y. Lee, J. C. Scott, R. D. Miller, Macromolecules **31**, 1099 (1998).
[18] M. Inbasekaran, E. P. Woo, W. Wu, M. Bernius, L. Wujkowski, Synth. Met. **111-112**, 397 (2000).
[19] N. S. Cho, J. H. Park, H.K. Shim, Curr. Appl. Phys. **6**, 686 (2006).
[20] C. Liu, X. Zou, S. Yin, W. Zhang, Thin Solid Films **466**, 279 (2004).
[21] T. Q. Nguyen, R. C. Kwong, M. E. Thompson, B. J. Schwartz, Appl. Phys. Lett. **76**, 2454 (2000).
[22] T. Q. Nguyen, V. Doan, B. J. Schwartz, J. Chem. Phys. **110**, 4068 (1999).
[23] R. Katoh, S. Sinha, S. Murate, M. Tachiya, J. Photochem. Photobiol. **A 145**, 23 (2001).
[24] C. M. Hsu, W. T. Wu, H. H. Lee, Displays **29**, 268 (2008).
[25] W. J. Lee, Y. K. Fang, H. C. Chiang, S. F. Ting, S. F. Chen, W. R. Chang, C. Y. Lin, T. Y. Lin, W. D. Wang, S. C. Hou, J. J Ho, Solid-State Electron. **47**, 927 (2003).

[26] I. W. Wu, Y. H. Chen, P. S. Wang, C. G. Wang, S. H. Hsu, C. I. Wu, Appl. Phys. Lett. **96**, 013301 (2010).
[27] X. J. Wang, J. M. Zhao, Y. C. Zhou, X. Z. Wang, S. T. Zhang, Y. Q. Zhan, Z. Xu, H. J. Ding, G. Y. Zhong, H. Z. Shi, Z. H. Xiong, Y. Liu, Z. J. Wang, E. G. Obbard, X. M. Ding, J. Appl. Phys. **95**, 3828 (2004).
[28] G. H. Xie, Y. L. Meng, F. M. Wu, C. Tao, D. D. Zhang, M. J. Liu, Q. Xue, W. Chen, Y. Zhao, Appl. Phys. Lett. **92**, 093305 (2008).
[29] J. Kim, J. Lee, C. W. Han, N. Y. Lee, I. J. Chung, Appl. Phys. Lett. **82**, 4238 (2003).
[30] C. H. Chou, C. F. Shu, Macromolecules **35**, 9673 (2002).
[31] G. Greczynski, M. Fahlman, W. R. Salaneck, Appl. Surf. Sci. **166**, 380 (2000).
[32] Y. D. Jin, X. B. Ding, J. Reynaert, V. I. Arkhipov, G. Borghs, P. L. Heremans, M. V. der Auweraer, Org. Electron. **5**, 271 (2004).
[33] Y. Q. Li, M. K. Fung, Z. Y. Xie, S. T. Lee, L. S. Hung, J. M. Shi, Adv. Mater. **14**, 1317 (2002).

*Corresponding author: shya@cc.kuas.edu.tw